10. R. Baradaran, J. M. Berrisford, G. S. Minhas, L. A. Sazanov, *Nature* **494**, 443–448 (2013).
11. R. G. Efremov, L. A. Sazanov, *Nature* **476**, 414–420 (2011).
12. C. C. Page, C. C. Moser, X. Chen, P. L. Dutton, *Nature* **402**, 47–52 (1999).
13. C. Hunte *et al.*, *Nature* **435**, 1197–1202 (2005).
14. E. Screpanti, C. Hunte, *J. Struct. Biol.* **159**, 261–267 (2007).
15. N. J. Hu, S. Iwata, A. D. Cameron, D. Drew, *Nature* **478**, 408–411 (2011).
16. V. K. Moparthi *et al.*, *Biochim. Biophys. Acta* **1837**, 178–185 (2014).
17. K. R. Vinothkumar, J. Zhu, J. Hirst, *Nature* **515**, 80–84 (2014).
18. B. C. Marreiros, A. P. Batista, A. M. Duarte, M. M. Pereira, *Biochim. Biophys. Acta* **1827**, 198–209 (2013).
19. R. G. Efremov, L. A. Sazanov, *Nature* **476**, 414–420 (2011).
20. A. Galkin, S. Dröse, U. Brandt, *Biochim. Biophys. Acta* **1757**, 1575–1581 (2006).
21. N. Kashani-Poor, K. Zwicker, S. Kerscher, U. Brandt, *J. Biol. Chem.* **276**, 24082–24087 (2001).
22. H. Jörnvall *et al.*, *Biochemistry* **34**, 6003–6013 (1995).
23. A. Abdrakhmanova, K. Zwicker, S. Kerscher, V. Zickermann, U. Brandt, *Biochim. Biophys. Acta* **1757**, 1676–1682 (2006).
24. M. Ciano, M. Fuszard, H. Heide, C. H. Botting, A. Galkin, *FEBS Lett.* **587**, 867–872 (2013).
25. V. Zickermann *et al.*, *J. Biol. Chem.* **278**, 29072–29078 (2003).
26. V. Zickermann, B. Barquera, M. Wikström, M. Finel, *Biochemistry* **37**, 11792–11796 (1998).
27. H. Angerer *et al.*, *Biochim. Biophys. Acta* **1817**, 1776–1784 (2012).
28. J. G. Okun, P. Lümmen, U. Brandt, *J. Biol. Chem.* **274**, 2625–2630 (1999).
29. M. A. Tocilescu *et al.*, *Biochim. Biophys. Acta* **1797**, 625–632 (2010).
30. M. A. Tocilescu, U. Fendel, K. Zwicker, S. Kerscher, U. Brandt, *J. Biol. Chem.* **282**, 29514–29520 (2007).
31. U. Fendel, M. A. Tocilescu, S. Kerscher, U. Brandt, *Biochim. Biophys. Acta* **1777**, 660–665 (2008).
32. A. B. Kotlyar, A. D. Vinogradov, *Biochim. Biophys. Acta* **1019**, 151–158 (1990).
33. E. Maklashina, A. B. Kotlyar, G. Cecchini, *Biochim. Biophys. Acta* **1606**, 95–103 (2003).
34. E. T. Chouchani *et al.*, *Nat. Med.* **19**, 753–759 (2013).
35. A. Galkin *et al.*, *J. Biol. Chem.* **283**, 20907–20913 (2008).
36. U. Brandt, *Biochim. Biophys. Acta* **1807**, 1364–1369 (2011).
37. L. Euro, G. Belevich, M. I. Verkhovsky, M. Wikström, M. Verkhovskaya, *Biochim. Biophys. Acta* **1777**, 1166–1172 (2008).
38. M. Babot *et al.*, *Biochim. Biophys. Acta* **1837**, 929–939 (2014).
39. V. R. Kaila, M. Wikström, G. Hummer, *Proc. Natl. Acad. Sci. U.S.A.* **111**, 6988–6993 (2014).

ACKNOWLEDGMENTS

Supported by the German Research Foundation (CRC 746 to C.H.; ZI 552/3-1 to V.Z.) and the Excellence Initiative of the German Federal and State Governments (EXC 115 to H.S., U.B., and V.Z.; EXC 294 BIOSS to C.H.). We thank the Swiss Light Source and European Synchrotron Radiation Facility for beamline access and staff support during visits, and A. Duchene and G. Beyer for excellent technical assistance. Coordinates and structure factors are deposited in the Protein Data Bank with accession code 4wz7.

SUPPLEMENTARY MATERIALS

www.sciencemag.org/content/347/6217/44/suppl/DC1
Materials and Methods
Figs. S1 to S11
Tables S1 to S3
References (*40*–*58*)

11 August 2014; accepted 1 December 2014
10.1126/science.1259859

ORGANIC CHEMISTRY

Nanomole-scale high-throughput chemistry for the synthesis of complex molecules

Alexander Buitrago Santanilla,[1] Erik L. Regalado,[1] Tony Pereira,[2] Michael Shevlin,[1] Kevin Bateman,[2] Louis-Charles Campeau,[1] Jonathan Schneeweis,[3] Simon Berritt,[1] Zhi-Cai Shi,[4] Philippe Nantermet,[5] Yong Liu,[1] Roy Helmy,[1] Christopher J. Welch,[1] Petr Vachal,[6] Ian W. Davies,[1] Tim Cernak,[7]* Spencer D. Dreher[1]*

At the forefront of new synthetic endeavors, such as drug discovery or natural product synthesis, large quantities of material are rarely available and timelines are tight. A miniaturized automation platform enabling high-throughput experimentation for synthetic route scouting to identify conditions for preparative reaction scale-up would be a transformative advance. Because automated, miniaturized chemistry is difficult to carry out in the presence of solids or volatile organic solvents, most of the synthetic "toolkit" cannot be readily miniaturized. Using palladium-catalyzed cross-coupling reactions as a test case, we developed automation-friendly reactions to run in dimethyl sulfoxide at room temperature. This advance enabled us to couple the robotics used in biotechnology with emerging mass spectrometry–based high-throughput analysis techniques. More than 1500 chemistry experiments were carried out in less than a day, using as little as 0.02 milligrams of material per reaction.

High-throughput experimentation (HTE) chemistry tools have been used to aid in the discovery of new reactions (*1*–*6*) and in the scale-up optimization of known reactions (*7*–*9*), both areas where substrates for experimentation are plentiful. However, HTE is rarely used in the area where it might have the greatest impact: the synthesis of complex natural products or highly functionalized drug leads. What is needed is a tool that would allow chemists to locate successful reaction conditions (*10*) on a microgram (nanomole) scale in a high-throughput fashion without depleting precious substrate stores.

In the search for breakthrough medicines in biomedical research, the rapid preparation of new, complex molecules for biological evaluation is of paramount importance, but substrates for the synthesis of such compounds are invariably in short supply. In later stages of chemistry development, substrates are abundant, and state-of-the-art microvial (*8*, *9*) or microfluidic (*11*) HTE tools can be effective in "turning on" reactions that were otherwise unsuccessful by exploring combinations of catalysts, reagents, and other key reaction variables (*12*, *13*). Such studies require at least milligram (micromole) quantities of substrate per reaction—a prohibitively large amount in early drug discovery, where new molecules are prepared for the first time. Consequently, the set of desirable compounds designed to test a biological hypothesis is often winnowed to the much smaller subset of compounds that can be successfully synthesized using a single set of reaction conditions, with little opportunity to study and improve unsuccessful syntheses (*14*, *15*). Miniaturizing chemistry to the nanomole scale is a potential solution to this problem that has heretofore met with substantial engineering problems, such as accurately bringing together extremely small charges of materials that are often heterogeneous, effectively agitating reaction mixtures, preventing loss of volatile solvents, and incorporating general analytical approaches to assay reaction outcomes. We present the first results of a study aimed at developing general nanomole reaction screening capabilities to support the rapid synthesis of complex, highly functionalized drug leads.

Figure 1A shows highly functionalized molecules from Merck's compound collection representative of the cores of drug molecules (**1** to **8**), which in the search for new molecules with optimal biological properties would be coupled to a diversity of polar building blocks (**9** to **20**) such as those in Fig. 1B. Modern organic synthesis (and especially transition metal catalysis) is redefining the rules with which new bonds can be forged; however, it is important to recognize that many "solved" synthetic transformations are far from universal, performing well on simple model substrates yet often failing when applied to complex substrates in real-world synthesis (*16*). A recent analysis of 2149 metal-catalyzed C-N

[1]Department of Process and Analytical Chemistry, Merck Research Laboratories, Merck and Co. Inc., Rahway, NJ 07065, USA. [2]Department of Pharmacokinetics, Pharmacodynamics and Drug Metabolism, Merck Research Laboratories, Merck and Co. Inc., West Point, PA 19486, USA. [3]Department of Pharmacology, Merck Research Laboratories, Merck and Co. Inc., Kenilworth, NJ 07033, USA. [4]Department of Discovery Chemistry, Merck Research Laboratories, Merck and Co. Inc., Kenilworth, NJ 07033, USA. [5]Department of Discovery Chemistry, Merck Research Laboratories, Merck and Co. Inc., West Point, PA 19486, USA. [6]Department of Discovery Chemistry, Merck Research Laboratories, Merck and Co. Inc., Rahway, NJ 07065, USA. [7]Department of Discovery Chemistry, Merck Research Laboratories, Merck and Co. Inc., Boston, MA 02115, USA.
***Corresponding author. E-mail: timothy_cernak@merck.com (T.C.); spencer_dreher@merck.com (S.D.D.)**

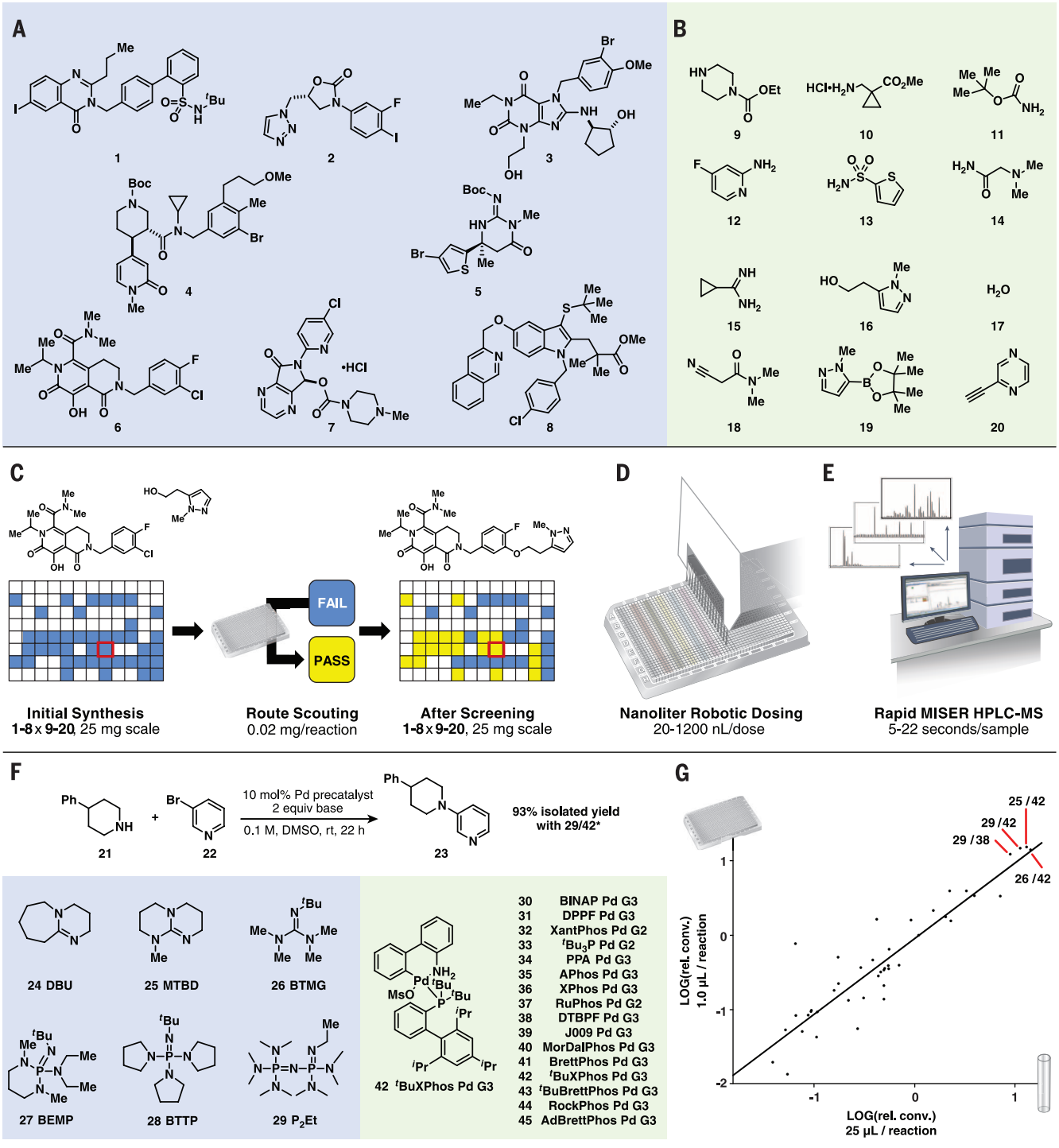

Fig. 1. Nanomole-scale reaction screening. (**A**) High-complexity electrophilic cores **1** to **8** from the Merck compound collection. (**B**) High-polarity nucleophilic building blocks **9** to **20**. (**C**) Route scouting to identify successful reaction conditions for previously failed chemistry can be accomplished using nanomole-scale reaction screening with minimal consumption of precious substrate (0.02 mg per reaction). Successful reactions run on nanoscale (0.02 mg, 50 nmol) can be repeated on a 25-mg scale (factor of 1000 scale-up). A 96-member parallel coupling library using best reaction conditions located by screening model nucleophiles (table S3) gave 54 products (white squares) and 42 failed reactions (blue squares) (table S4). After nanomole-scale screening, productive conditions were located for an additional 21 of the 96 products (yellow squares) (tables S6 and S8). (**D**) Reaction mixtures that are fully soluble in high-boiling solvents can be dosed with high-precision nanoliter robotics. Room-temperature reactions require no stirring and minimal sealing. (**E**) High-performance LC-MS MISER analysis allows for rapid label-free analysis of reactions with diverse products. (**F**) Reaction discovery: Organic superbases **24** to **29** promote room-temperature cross-coupling in DMSO with second- and third-generation biaryl palladium precatalysts **30** to **45**. (**G**) Ninety-six combinations of bases and ligands were investigated in triplicate in glass microvials with stirring and reproduced in 1536-well plastic microtiter plates without stirring.

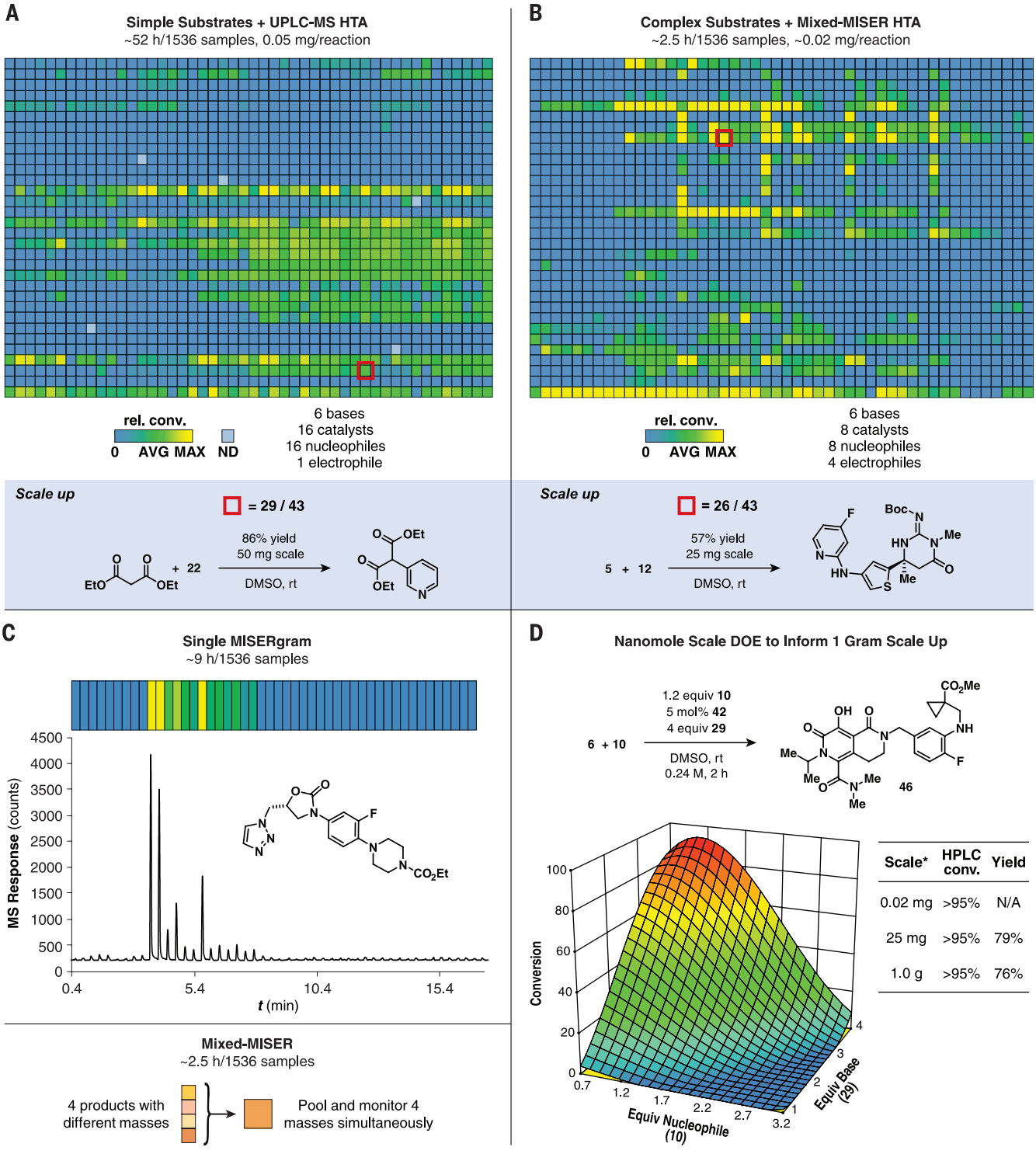

Fig. 2. A high-throughput nanomole-scale chemistry evaluation using rapid MISER and mixed-MISER LC-MS. (**A**) Heat map showing data from 1536 nanomole-scale reactions analyzed by UPLC (total analysis time ~52 hours). Sixteen diverse N/C/O/P/S nucleophiles were screened against 96 catalyst-base combinations to find room-temperature coupling conditions to 3-bromopyridine **22**. Best conditions for each nucleophile were repeated on a 50-mg scale, giving 68 to 95% isolated yields (table S3). Reaction information about best catalyst-base combination was matched to the polar nucleophile used in the 96-member parallel coupling library of **1** to **8** × **9** to **20** (Fig. 1C, initial synthesis). (**B**) Heat map showing data from 1536 nanomole-scale reactions analyzed by MISER. Thirty-two electrophile-nucleophile combinations that failed under previous best conditions were investigated under 48 catalyst-base combinations. Best conditions for each combination were repeated on a 50-μmol scale and assigned a "PASS" (Fig. 1C, after screening) if a >95% purity sample was obtained. (**C**) MISER chromatographic output (MISERgram) for 48 catalyst-base combinations that were screened with 0.02 mg of **2** per reaction, using **9** as nucleophile, and depiction of pooled MISER approach. (**D**) Nanomole-scale DOE: three-factorial, four-level DOE surface model produced by screening **6** against reagent charges of **10**, **29**, and **42**. *Conditions identified in 0.02 mg scale reactions informed practical 25-mg and 1-g scale-ups.

couplings run in the final steps of the synthesis of highly functionalized drug leads revealed that 55% of reactions failed to deliver any product at all (*17*). The missed opportunity represented by these unsuccessful syntheses haunts contemporary drug discovery, and there is a growing recognition that the tendency of polar, highly functionalized compounds to fail in catalysis may actually enrich compound sets in hydrophobic molecules that are less likely to become successful drug candidates (*15*, *16*, *18*–*20*).

Soluble superbase coupling conditions for miniaturization from micromole to nanomole scale

Using the catalysis cross-coupling space defined in Fig. 1, A and B, as a test case, this work evaluates the idea that miniaturized chemistry experimentation to inform preparative scale synthesis (Fig. 1C) could be run on the same scale as contemporary biological assays using the high-precision nanoliter robotics commonly used in biochemistry labs (Fig. 1D) in conjunction with high-throughput mass spectrometric analysis (Fig. 1E). The engineering complexities of this task could potentially be overcome by using ambient-temperature chemistry that operates in a solubilizing, low-volatility, plastic-compatible reaction medium such as dimethyl sulfoxide (DMSO) or *N*-methyl-2-pyrrolidone (NMP). We chose DMSO for the initial proof of concept because it is an environmentally friendly solvent and represents the potential to directly link chemistry with biochemical experimentation. Very few efficient ambient-temperature palladium-catalyzed cross-couplings in DMSO or other polar solvents have been reported (*21*), in part because of the strong solvent-metal coordination of such solvents and their incompatibility with the strong bases typically used in low-temperature C-N couplings (NaO^tBu, $LiN(SiMe_3)_2$, $Zn(N(SiMe_3)_2)_2$ etc.) (*22*). It seemed possible that recently reported highly hindered, electron-rich ligands (*23*) may effectively protect Pd from DMSO coordination and that non-nucleophilic organic superbases (*24*), which are soluble in most solvents and should be strongly basic enough to promote Pd C-N couplings at room temperature, could be compatible with these solvents.

Initially working in glass microvials, which represent the current validated lower limits of scalable batch miniaturization (*8*, *9*), the coupling of amine **21** with bromide **22** (2.5 μmol in 25 μl of DMSO) was evaluated in a 96-reaction array of superbases **24** to **29** with catalysts **30** to **45** [10 mole percent (mol %)] (Fig. 1F), and several highly productive room-temperature coupling conditions were identified. All solutions were homogeneous but were stirred nonetheless. This same 96-reaction array was then evaluated on a 1.0-μl scale (100 nmol of substrate) in a plastic 1536-well plate without stirring and with reagent dosing via a nanoliter liquid-handling robot (TTP LabTech Mosquito HTS) inside a nitrogen-filled glovebox, demonstrating the same hits and reaction performance (Fig. 1G). The Mosquito robot allows sequential aspiration from different wells of a source plate into a single pipette tip to create multicomponent mixtures that are dosed as single reaction drops into a 1536-well plate. This ensures proper mixing of the reaction components and obviates the need for stirring. This pipetting mechanism, in conjunction with a material-sparing source plate with minimal dead volume, ensures that almost no material is wasted, and the overage can be recovered if desired. Also, with this batch reaction approach, some degree of sample heterogeneity can be tolerated, unlike for microfluidic technologies where channel clogging can lead to systemic failure.

The coupling of bromide **22** was then evaluated with 16 nitrogen, oxygen, carbon, phosphorus, and sulfur nucleophiles under the same 96 combinations of **24** to **45** in a single miniaturized 1536-reaction experiment (Fig. 2A and table S3). In this experiment, dosing required 30 min (four components per well, 6144 total reagent doses) followed by 22 hours of reaction time, 1 hour for automated reaction quenching and sampling, and 52 hours for analysis by ultra performance liquid chromatography (UPLC). This experiment uncovered extremely mild, soluble coupling conditions for amines, alcohols, amides, sulfonamides, carbamates, amidines, aryl boronates, alkynes, and malonates, most of which have not been reported at ambient temperature with non-nucleophilic bases (table S3). Because the reactions were by design homogeneous and required no heating or cooling, translation to a larger scale was straightforward, delivering 68 to 98% yield when scaled up by a factor of 3000, to 320 μmol of **22** (50 mg), now running at 5 mol % catalyst loading and 0.2 M substrate concentration.

Implementation of nanomole screening for complex molecule synthesis

These new coupling conditions were next applied in complex synthesis to the test set of electrophiles **1** to **8** and nucleophiles **9** to **20** (Fig. 1, A and B). Initial synthesis conditions for this array were selected from the best permutation of superbase and catalyst that was previously identified for each nucleophile class when using bromide **22** (table S3). With these conditions, high-purity product samples were successfully prepared for 54 of the 96 functionality-rich substrate combinations (Fig. 1C and table S4) when run on a 500-μmol scale (~25 mg) (*25*, *26*). This chemistry was generally tolerant of polar functional groups and heterocycles; however, nearly half of the 96 reactions failed to provide any product, which is typical for application of a single set of conditions to a complex catalysis problem.

To apply nanomole-scale reaction screening to this problem, we subjected 32 different electrophile-nucleophile substrate combinations, each of which produced little or no material from the 96-reaction array, to 48 reaction conditions (8 organic superbases × 6 ligands; Fig. 2B). The substrate concentration was reduced to 0.05 M and the catalyst loading was doubled to 20 mol % so that running all 48 reactions would consume less than 1 mg of each substrate (50 nmol, ~0.02 mg per reaction) (*27*). In addition, the reaction time was reduced to 2 hours and a faster liquid chromatography–mass spectrometry (LC-MS) approach was pursued, with a goal of running and analyzing 1536 reactions in less than 24 hours. Of the available label-free techniques (*28*), MISER (multiple injections in a single experimental run) LC-MS was selected for its ease of data acquisition and analysis (*29*). Thus, 48 reactions that had the same potential product along a row of the 1536-well plate were analyzed by multiple injections (22 s per sample) in a single isocratic chromatographic run with mass detection settings observing the molecular ion for the desired product (Fig. 2C). In this way, the 1536-well plate could be analyzed in ~9 hours. To reduce the time required for analysis even further, we combined four rows of reaction samples that could give different product masses and simultaneously monitored the four desired products' *m/z* values (mass/charge ratios) in these pooled samples (Fig. 2C). By pooling four mass-encoded wells, the analysis of all 1536 reactions could be performed in ~2.5 hours. In addition, a more rigorous approach to this same analysis was pursued using a parallel two-channel LC system connected to a triple-quadrupole mass spectrometer. This instrumentation used a fast gradient to provide improved resolution and additional MS/MS structure confirmation data and required ~2.5 hours for analysis of all 1536 reactions. The MISER analyses located the expected product masses for 21 of 32 substrate combinations, and the best hits were then confirmed with UPLC-MS. These 21 hits were scaled up by a factor of 1000 (25-mg scale), and a pure product sample was obtained for 16 of these reactions (table S6).

Optimization of continuous variables (for example, the stoichiometry of reagents) is another potential path to increase product formation in HTE. Returning to the conditions originally identified for bromide **22**, six of the remaining failed reactions were evaluated under 48 combinations of catalyst loading, nucleophile charge, and base charge, again using 1 mg of substrate per 48-reaction evaluation (fig. S22). Markedly better conditions for five of the six compounds were found in this way, which allowed their isolation upon scale-up by a factor of 1000 (table S8). Hence, in these two miniaturized screening experiments, looking first at catalyst-base combinations and then at reaction stoichiometries, 21 complex new compounds could be rapidly prepared. These solutions to 21 complex synthesis problems represent the opportunity to answer biological hypotheses that would have been passed over in previous chemistry approaches because of lack of time and material.

Nanomole reaction optimization to inform gram-scale synthesis

An important consideration for this nanomole-scale approach toward discovery synthesis is the optimization of reactions for application to larger-scale synthesis. Compounds that are deemed interesting in initial biological evaluation or are synthetic intermediates in a multistep route must rapidly be prepared in larger quantities once conditions are identified. Statistical tools such

as DOE (design of experiments) are powerful tools for synthesis (*30*–*32*), yet they typically focus on performing minimal numbers of experiments, as large numbers of experiments are often resource- and time-intensive to conduct. However, because large numbers of experiments are readily feasible with this nanomole-scale chemistry platform, we were able to construct a three-factorial, four-level response surface modeling experiment to study the loading of catalyst against varying stoichiometries of base and nucleophile in the reaction of chloride **6** with amine **10**. In this DOE experiment, each condition was repeated twice, resulting in 128 total reactions with <3 mg of **6**. Indeed, a high-quality response surface model was generated with the nanomole-scale chemistry approach (Fig. 2D), which helped to define the critical charges of nucleophile and base for optimal reaction performance. The optimized conditions used 15 mol % **42** at 0.05 M concentration; by translating to more practical conditions of 5 mol % **42** and 0.24 M concentration, we obtained full conversion and a 79% isolated yield of **46** on a 25-mg scale, which was reproduced to obtain a 76% isolated yield on a 1-g scale (Fig. 2D). This result shows that advanced statistical reaction analysis, which is typically reserved for chemistry opportunities where material is plentiful, can be applied to reactions in the material-limited front lines of drug discovery or natural product synthesis.

In biomedical research, chemical synthesis should not limit access to any molecule that is designed to answer a biological question. This work demonstrates an example of how conditions for complex Pd-catalyzed C-O, C-N, and C-C cross-coupling reactions can be evolved into a powerful, substrate-focused approach to chemistry miniaturization to overcome limited access to complex products. With innovative research, other high-value modern chemistry reactions could be similarly designed into this paradigm to improve synthesis in material-limited environments by evolution of catalysts and reagents to perform in DMSO, NMP, or other high-boiling solvents at ambient temperature.

REFERENCES AND NOTES

1. M. R. Friedfeld *et al.*, *Science* **342**, 1076–1080 (2013).
2. D. A. DiRocco *et al.*, *Angew. Chem. Int. Ed.* **53**, 4802–4806 (2014).
3. D. W. Robbins, J. F. Hartwig, *Science* **333**, 1423–1427 (2011).
4. A. McNally, C. K. Prier, D. W. C. MacMillan, *Science* **334**, 1114–1117 (2011).
5. K. D. Collins, T. Gensch, F. Glorius, *Nat. Chem.* **6**, 859–871 (2014).
6. R. Moreira, M. Havranek, D. Sames, *J. Am. Chem. Soc.* **123**, 3927–3921 (2001).
7. S. M. Preshlock *et al.*, *J. Am. Chem. Soc.* **135**, 7572–7582 (2013).
8. A. Bellomo *et al.*, *Angew. Chem. Int. Ed.* **51**, 6912–6915 (2012).
9. J. R. Schmink, A. Bellomo, S. Berritt, *Aldrichim. Acta* **46**, 71–80 (2013).
10. M. Peplow, *Nature* **512**, 20–22 (2014).
11. T. Rodrigues, P. Schneider, G. Schneider, *Angew. Chem. Int. Ed.* **53**, 5750–5758 (2014).
12. S. Monfette, J. M. Blacquiere, D. E. Fogg, *Organometallics* **30**, 36–42 (2011).
13. P. M. Murray, S. N. G. Tyler, J. D. Moseley, *Org. Process Res. Dev.* **17**, 40–46 (2013).
14. S. D. Roughley, A. M. Jordan, *J. Med. Chem.* **54**, 3451–3479 (2011).
15. T. W. J. Cooper, I. B. Campbell, S. J. F. Macdonald, *Angew. Chem. Int. Ed.* **49**, 8082–8091 (2010).
16. A. Nadin, C. Hattotuwagama, I. Churcher, *Angew. Chem. Int. Ed.* **51**, 1114–1122 (2012).
17. Merck internal study of electronic notebooks.
18. M. M. Hann, G. M. Keserü, *Nat. Rev. Drug Discov.* **11**, 355–365 (2012).
19. F. Lovering, J. Bikker, C. Humblet, *J. Med. Chem.* **52**, 6752–6756 (2009).
20. H. A. Malik *et al.*, *Chem. Sci.* **5**, 2352–2361 (2014).
21. R. E. Tundel, K. W. Anderson, S. L. Buchwald, *J. Org. Chem.* **71**, 430–433 (2006).
22. D. S. Surry, S. L. Buchwald, *Chem. Sci.* **2**, 27–50 (2011).
23. N. C. Bruno, M. T. Tudge, S. L. Buchwald, *Chem. Sci.* **4**, 916–920 (2013).
24. T. Ishikawa, Y. Kondo, H. Kotsuki, T. Kumamoto, D. Margetic, K. Nagasawa, W. Nakanishi, in *Superbases for Organic Synthesis: Guanidines, Amidines, Phosphazenes and Related Organocatalysts*, T. Ishikawa, Ed. (Wiley, West Sussex, UK, ed. 1, 2009), pp. 1–326.
25. Compounds were generally purified by MS-directed purification. Isolated yields ranged from 1 to 100%, but we made no attempt to maximize the isolated yields in these reactions and instead focused on obtaining high-purity compounds as quickly as possible, which is typical in most medicinal chemistry campaigns. Some reactions showed product formation by UPLC-MS analysis but were either insufficiently pure or too low in yield for purification.
26. M. Liu *et al.*, *ACS Comb. Sci.* **14**, 51–59 (2012).
27. Some electrophiles were not fully soluble in DMSO, so NMP was used instead. Even though three stock solutions in NMP still displayed mild insolubility, the TTP Mosquito operates on positive-displacement pipetting, so viscous solutions or suspensions of small particulates are easily transferred.
28. W. Schafer, X. Bu, X. Gong, L. A. Joyce, C. J. Welch, in *Comprehensive Organic Synthesis*, C. J. Welch, Ed. (Elsevier, Oxford, ed. 2, 2014), vol. 9, pp. 28–53.
29. C. J. Welch *et al.*, *Tetrahedron Asymmetry* **21**, 1674–1681 (2010).
30. J. C. Ianni, V. Annamalai, P.-W. Phuan, M. Panda, M. C. Kozlowski, *Angew. Chem. Int. Ed.* **45**, 5502–5505 (2006).
31. S. E. Denmark, C. R. Butler, *J. Am. Chem. Soc.* **130**, 3690–3704 (2008).
32. K. C. Harper, M. S. Sigman, *Science* **333**, 1875–1878 (2011).

ACKNOWLEDGMENTS

We thank S. Krska, M. Tudge, G. Hughes, and E. Parmee for helpful discussions; M. Liu, E. Streckfuss, T. Meng, N. Pissarniski, and W. Li for assistance in purification of compounds; M. Christensen and J. Voigt for experimental assistance; and S. M. O'Brien and M. McColgan for graphic design. S.B. was supported by an NSF GOALI Grant associated with the University of Pennsylvania. Supported by the MRL Postdoctoral Research Fellows Program (A.B.S. and E.L.R.).

SUPPLEMENTARY MATERIALS

www.sciencemag.org/content/347/6217/49/suppl/DC1
Materials and Methods
Supplementary Text
Figs. S1 to S32
Tables S1 to S11
References (*33*–*40*)
Data Files S1 to S5

25 July 2014; accepted 11 November 2014
Published online 20 November 2014;
10.1126/science.1259203

REPORTS

QUANTUM OPTICS

Quantum harmonic oscillator state synthesis by reservoir engineering

D. Kienzler,* H.-Y. Lo, B. Keitch, L. de Clercq, F. Leupold, F. Lindenfelser, M. Marinelli, V. Negnevitsky, J. P. Home*

The robust generation of quantum states in the presence of decoherence is a primary challenge for explorations of quantum mechanics at larger scales. Using the mechanical motion of a single trapped ion, we utilize reservoir engineering to generate squeezed, coherent, and displaced-squeezed states as steady states in the presence of noise. We verify the created state by generating two-state correlated spin-motion Rabi oscillations, resulting in high-contrast measurements. For both cooling and measurement, we use spin-oscillator couplings that provide transitions between oscillator states in an engineered Fock state basis. Our approach should facilitate studies of entanglement, quantum computation, and open-system quantum simulations in a wide range of physical systems.

Reservoir engineering is a method in which specially designed couplings between a system of interest and a zero-temperature environment can be used to generate quantum superposition states of the system as the steady state of the dissipative process, independent of the initial state of the system (*1*–*3*). Theoretical work has shown the potential for using such engineered dissipation for universal quantum computation (*4*) and in providing new routes to many-body states (*5*–*7*). Experimentally, these techniques have been used to generate entangled superposition states of qubits in atomic ensembles (*8*), trapped ions (*9*, *10*), and superconducting circuits (*11*). Theoretical proposals for quantum harmonic oscillator state synthesis by reservoir engineering extend from trapped ions (*2*, *3*) to superconducting cavities (*12*, *13*) and nanomechanics (*14*).

Here, we experimentally demonstrate the generation and stabilization of quantum harmonic oscillator states by reservoir engineering based on the original proposal of Cirac *et al.* (*1*), which we use to generate and stabilize squeezed,

Institute for Quantum Electronics, ETH Zürich, Otto-Stern-Weg 1, 8093 Zürich, Switzerland.
***Corresponding author. E-mail: daniel.kienzler@phys.ethz.ch (D.K.); jhome@phys.ethz.ch (J.P.H.)**

Editor's Summary

Breaking through the milligram floor

When chemists synthesize compounds, the threshold for success is at least a milligram of product. This has been true for decades—even though biochemical assays have long since descended into microgram territory—and results in part from the constraints of characterization methods. Buitrago Santanilla *et al.* present an automated dosing and characterization protocol for optimizing chemical reaction conditions on the microgram scale. This allowed them to screen numerous base and ligand combinations for catalytic C-N bond-forming reactions between complex pairs of compounds, in short supply, that resisted standard coupling conditions.

Science, this issue p. 49